Multimedia Tools and Applications (2024) 83:37795–37812
https://doi.org/10.1007/s11042-023-16725-8

An efficient image compression using modified embedded zero tree coding with SVD

R Naveen Kumar[1]

Received: 24 October 2022 / Revised: 16 July 2023 / Accepted: 31 August 2023 /
Published online: 2 October 2023

Abstract
The fast-growing web technology is more focused on developing optimized image compression tools to increase the efficiency of search engines and data validation. The wavelet-based progressive image compression is a more popular compression technique used in standard JPEG 2000 codec design for multimedia image applications. The embedded zero tree wavelet coding (EZTW) is one of the lossy wavelet-based image compression which produces a high compression rate by neglecting redundant coefficients during encoding. However, singular value decomposition (SVD) is a lossless image compression, where high energy compaction and adaptability for local variance made its reconstruction quality high with a shortcoming compression ratio. In this proposed hybrid technique, the mean extracted image is segmented into blocks were subjected to SVD and modified EZTW compression. In addition, adaptive thresholding and rank selections by using an optimizer algorithm help in scoring high compression rates and effective edge reconstruction. The comparative study of the proposed technique with the art of work shows an enhancement in PSNR scores, significantly obtained at 24.64 dB even at high compression rates (90:1) for boat images.

Keywords Image compression · singular value decomposition (SVD) · modified embedded zero-tree wavelet (MEZTW)

1 Introduction

Internet usage has become a vital part of our daily life and almost two third of the global population is interconnected with web applications [1]. The web-based devices such as smartphones and tablets influence each individual connected across the world and upraise the demand for designers to develop advanced data processing tools [2]. In general, web contents include high-resolution images, text, audio, and video data which are larger in volume and require more transmission time for its communication. Image compression

✉ R Naveen Kumar
nkr.hsd@gmail.com

[1] Department of Electronics, M S Ramaiah College of Arts, Science and Commerce, Bengaluru, Karnataka 560054, India

is a conventional method to reduce the size of data without disturbing the architecture of the system [3]. The wavelet-based progressive image compression is one of the prominent algorithms used in current compression technology available in both lossy and lossless methods [4].

Motivation Even substantial wavelet methods are effective in high-quality reconstruction despite having limitations on storage and transmission bandwidth. The ability of feature extraction in JPEG 2000 from the region of interest dealt with compression ratio, even at low bandwidth transmission is quite impressive and made this codec ideal for internet/network applications. Hence, revisiting the old compression algorithm and reducing all its constraints for generating the best possible image quality reconstruction with a high transmission rate is a rousing step in compression technology.

Problem Statement Shapiro's Embedded Zero Tree Wavelet coding (EZTW) provides tunable resolution in embedded bit stream with wider dynamic range, and less error [5]. However, they consume a lot of computer processing power and provide the best results. There is a tradeoff in achieving quality reconstruction at dynamic range and no such tuning options for quality enhancement. Achieving low bit rate transmission, high compression ratio, and preservation of image quality during reconstruction are the key factors we are focusing on in this work.

Literature review The quest for efficient lossless image coding is always critical at low bandwidth transmission in network applications. The spatial-based image compression is a very primitive method, achieving compression either by eliminating the recursive pixels or by predicting the neighborhood pixels in adaptive lossless compression [6]. The multiresolution property of wavelet transform made it a robust compression algorithm in identifying redundant sub-bands and their removal [7]. The multiresolution scaling and adaptive thresholding property in Wavelet transform for image reconstruction made remarkable changes in image compression technology. The JPEG and JPEG2000 are prominent compression standards that use discrete cosine and wavelet transforms as conventional methods for image compression [8, 9]. JPEG compression has the substantial disadvantage of blocking artifacts and information reliance in an Image [10]. The EZTW is an efficient wavelet-based image compression that produces a fully embedded bitstream with high compression performance [5]. Later, much revolutionary research happened in compression coding using the EZTW algorithm, which includes Set Partition Hierarchical Tree (SPIHT), Embedded Block Coding Technique (EBCOT), Wavelet Difference Reduction (WDR), and Advanced WDR (ASWDR) [11–15]. Many attempts were made to hybridize the EZWT algorithm to reduce its constraints and enhance the compression performance suggested in the literature [16–20]. In [21], the author proposed a hybrid image compression algorithm that uses WDR with SVD followed by resolution enhancement using stationary wavelet transform (SWT) and discrete wavelet transform (DWT). Whereas, the low-frequency sub-band is decoded by inverse WDR and the high-frequency sub-band by matrix multiplication. As a result, the quality of a reconstructed image is significantly improved with a reduced embedded bit stream. In [22], a blended compression algorithm using SPIHT with SVD retains image quality by effective edge reconstruction and block-based SVD for low-frequency sub-bands during reconstruction. With the above literature survey, we can say the hybridization of dynamic image compression with SVD will perhaps improve the compression performance.

Contribution This proposed work made an effort to enhance the traditional EZTW algorithm by using Segmentation based adaptive EZTW with SVD for tunable compression rates. In this algorithm, compression speed is increased by increasing the correlation between wavelet coefficients and dividing the entire image into small chunks, and then compressing it into an embedded bit stream. In SVD, the distribution of singular values and their percentage of ranks are augmented by an optimizing algorithm. Meantime, adaptive EZTW compresses the image with an optimal threshold value targeting edge recovery. This hybrid algorithm found significant improvement in terms of PSNR and tested with standard test images and compared with Basic EZTW with Huffman coding, SPIHT, and JPEG.

This paper is organized as follows: proposed hybrid compression algorithm is explained in section II. Section III describes the functional block of the proposed hybrid compression method. The quality metrics, experimental outcomes, and result analysis are explained in sections IV, V then followed by a conclusion in section VI.

2 The proposed hybrid compression algorithm

In this proposed algorithm, the image is compressed in two different stages, using SVD and modified EZTW(MEZTW) as follows,

2.1 Compression using SVD

The general, SVD considers the image frame as a two-dimensional matrix of $\boldsymbol{m}$ x $\boldsymbol{n}$ pixels. Each pixel has its grey scale intensity ranging from 0 to 255. The SVD detaches the matrix into three product matrices $U\alpha V^T$, where **U** and **V** are the orthogonal matrices of m x n and n x n, respectively, and α is a non-negative and diagonal matrix of m x n [23]. Here compression is achieved by selecting the minimum number of ranks in the diagonal matrix to approximate the original image during the reconstruction process.

Here we refine the SVD in two additional steps:

- Calculate the mean value of the image matrix, then subtract the image matrix by its mean value before SVD and then add the mean value during reconstruction.
- Divide the mean extracted image matrix into sub-block to use the irregular density of the original image. Select the suitable percentage of the sum of the singular value instead of the predetermined value [24].

Consider for an image $\boldsymbol{J}$, the segmentation-based rank one SVD process is given by.

a. A matrix '$\boldsymbol{S}$' is obtained by subtracting the original image matrix '$\boldsymbol{J}$' from its mean value.

$$S(m,n) = J(m,n) - mean(J) \tag{1}$$

b. Define the block size (256×256,512×512……..) for segmentation.
c. Apply the forward SVD for each sub-blocks of matrix '$\boldsymbol{S}$' by using Eq.2.

$$\left[A_u, A_\alpha, A_v\right] = svd[S(m,n)] \tag{2}$$

Where Au is $m \times m$ matrix of orthogonal eigenvectors of $A \times A^T$, A_v is a transpose of is $n \times n$ matrix consisting of orthogonal eigenvectors of $A^T \times A$ and A_α is $m \times n$ diagonal matrix of singular values, square root of eigenvectors $A^T \times A$. Further, the average rank of matrix P is calculated from SVD by using some nonzero singular values in A_α.

d. The average rank matrix is calculated by using Eq. 3

$$P = \sum_{i=1}^{\min(m,n)} \propto_i u_i v_i \tag{3}$$

Where, $\propto_i$ is the i^{th} singular value and u_i, v_i are the corresponding left and right singular vectors.

e. The specific percentage of ranks is calculated by using Eq. 4 and Table 1

$$Specified\ percentage\left(S_p\right) = \frac{\left(p_1 + p_2 + p_3 + \ldots \cdots + p_k\right)}{\left(\sigma_1 + \sigma_2 + \sigma_3 + \ldots \cdots + \sigma_k\right)} \tag{4}$$

Where $'P_k'$ is the average rank matrix, $'\sigma_k'$ is a variance of singular values for each sub-blocks of the image.

Table 1 provides a piece of information on the selection of percentage rank, and singular value for block size 8×8 from updated singular values 25% to 85% (concerning edge preservation index).

f. Apply the Inverse SVD for reconstruction

$$B(m,n) = svd\left(Tu, T\alpha_{k1}, Tv\right) \tag{5}$$

Where, Tu is m by n, Tv is $K1$ by n, and $\alpha 1 = diag\,(r_1, r_2, r_3, \ldots, r_{k1})$

g. Recombine all sub-blocks to get ***S(m,n)***, then add the mean value to reconstruct the original image.

$$J^{-1}(m,n) = S(m,n) + mean(J) \tag{6}$$

*Rank one updated SVD exploits the distribution of singular values in the diagonal matrix. This singular value distribution varies along with image complexity.

Table 1 Average ranks and their percentage for given singular values of boat image

singular values	Avg. ranks	% of avg. ranks
95	1.000	0.125
85	1.000	0.125
70	1 .120	0.130
55	1 .022	0.127
25	2.340	0.134

2.2 Compression using MEZTW

The low bit rate is a major problem in EZTW coding because of scalar quantization which generates a sequence of zero and non-zero symbols [25, 26]. The probability of zeros in overall symbols is always high and so low bit rate transmission is difficult. But somehow it is possible by designing adaptive quantizers and encoders. A new modified adaptive threshold compression algorithm used in [27] shows a possible way for conserving the significant subband and killing unwanted zeroes in an embedded bit stream. It uses parent-child relations in decomposed wavelet coefficients using adaptive threshold and creates a new data structure with zero trees to encode the symbols.

The source image is decomposed by using pyramid decomposition [28] with Debauchee's wavelet filters at level 3 as shown in Fig. 1a. Scan the complete image by using raster scanning order then classify the coefficients as

a. Parent: Coefficients at crude decomposed scale. (Each parent has four offspring)
b. Child: Coefficients correspond to the same spatial location at the next bigger scale of parallel direction.
c. Descendent: Coefficients Child's offspring.

The initial threshold of EZTW is calculated by using the formula for decomposed wavelet coefficients ***I(m,n)***,

$$T_0 = \left[\log_2(\max(I))\right]^2 \tag{7}$$

Significance mapping If a wavelet coefficient 'z' is said to be significant if$|z| > T_0$, otherwise coefficient is considered insignificant. And also, symbols are classified as shown in Fig. 1b based on their status as follows,

- Zero tree roots: Coefficient and child are zero.

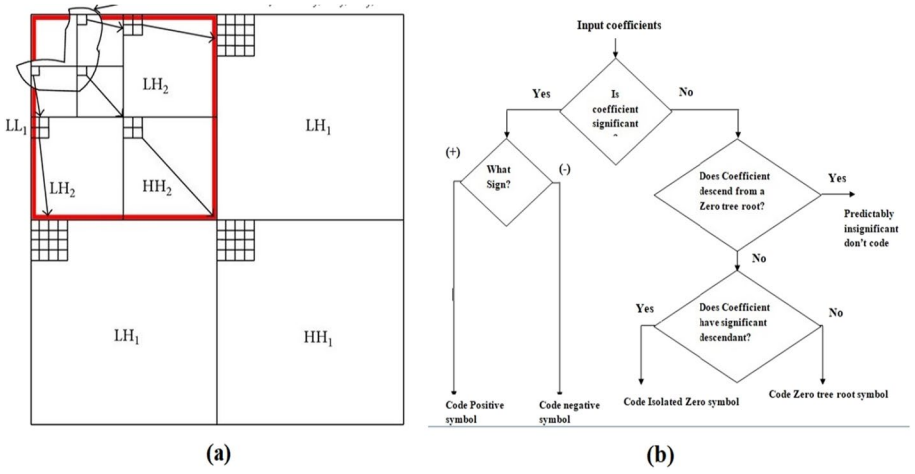

Fig.1 **a** Wavelet Pyramid decomposition of sub-band with parent-child relation; **b** flow of Significant mapping for wavelet coefficients

- Isolated Zero: The coefficient is insignificant but has significant descendants.
- Positive Significant: Coefficient values with a positive sign greater than the threshold value.
- Negative Significant: Coefficient values with a negative sign greater than the threshold value.

2.3 Optimizer for Adaptive threshold

A coarse compressed image is obtained from the first iteration with initial threshold and average ranks. The optimizer algorithm is designed in a way that image quality can be adopted by using a modified threshold value for required quality at a fixed compression ratio.

- The adaptive threshold for MEZTW is calculated by computing the median of the ordered list of reconstructed block coefficients φ using Eq.8.

$$T_{adp} = \begin{cases} \varphi\left[\frac{n+1}{2}\right] \; if\ n\ is\ odd \\ \frac{\varphi\left[\frac{n}{2}\right]+\varphi\left[\frac{n}{2}+1\right]}{2}, if\ n\ is\ even \end{cases} \tag{8}$$

  Whereas, $\boldsymbol{n}$ is the number of values of the data set from the reconstructed image. Then, carry out the significance test and repeat the process until the required bit rate is achieved. These symbols are encoded by a Huffman encoder, and finally, a lengthy compressed bit stream is obtained.
- With the help of a first-level reconstructed image, a specific percentage is normalized by Eq.9

$$S_P^+ = \sum \frac{(S_p - \varphi)}{S_{pmax} - S_{pmin}} \tag{9}$$

  then sort the ranks left to right based on significance $\left(S_{p1}^+ \geq S_{p2}^+ \geq \ldots\ldots.., S_{pmin}^+ \geq \ldots.0\right)$ and eliminate less significant specific ranks and apply for image blocks in the second iteration. The application of adaptive ranks is more effective in minimizing the noise and preserving the edge information in the image block.

3 Process flow of the proposed compression method

In this proposed method, the SVD compression is used for mean extracted source image blocks followed by the MEZTW encoder to get a compressed bit stream. Meantime, the optimizer calculates the average ranks and adaptive threshold value based on a reconstructed image in the first iteration to reduce the size of a bit stream. This process will continue until all blocks of the original image are compressed and reconstructed for a defined bit rate Fig. 2 and 3.

It takes the following steps,

a. **Preprocessing:** The original image is scaled down to standard size (1024×1024) to perform compression on a standard-size image. The mean subtraction method is the most common normalization process to increase inter-pixel relations and streamline

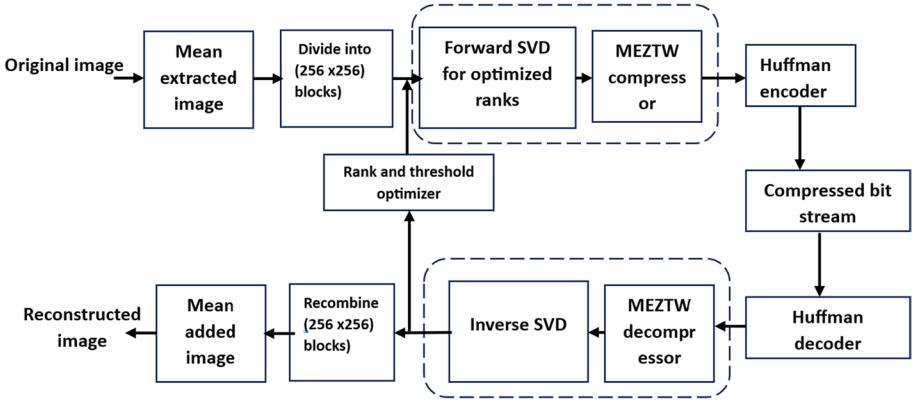

Fig. 2 Pipeline view of proposed MEZTW with SVD algorithm

the compression bit stream. The geometric interpretation is to Centre the significance pixels around the origin along each dimension by removing the mean across each unique feature in the image using Eq. 1.

b. Segment the image matrix into blocks of standard size (256×256 or 512×512). This step will help in increasing the coding efficiency of compressors.
c. **SVD Compression:** Apply SVD compression using Eq.2 and 4 with the application of adaptive ranks.
d. The application of MEZTW compression for given blocks:

Fig. 3 mean extracted blocks of Lena image

Let, B(m,n) = db4 wavelet coefficients of blocks

- l = *level of wavelet subtrees in a significant Mapping*
- $l\_\max$ = *maximum decomposition level of significant mapping*
- $Q_n(.)$ = *n bit linear quantizer*
- $AST\_Enc(.)$ = *Adaptive significant tree symbol encoder*
- ES = Encoded symbol.
- $K(m,n)$ = *Spatial oriented tree of root* $B(m,n)$
- P_3 = *subtree of* $K(m,n)$*at level* 3
- $\beta_s(m,n)$ = *Significant Coefficient of subtree* P_3
- $Z(m,n)$ = *encoded positions of* β_s

Step1: Calculate the minimum number of bits required to encode decomposed coefficients

$$n = \left\lceil \log_2\{\max|\mathrm{B}(m,n)|\}\right\rceil \tag{10}$$

Apply n-bit quantizer:

$$B_Q(m,n) = Q_n\{B(m,n)\} \tag{11}$$

Step2: Apply Adaptive threshold from eq.8.

Step3: Significant mapping:

calculate the db4 coefficient for given block B(m,n) in a raster scan order.

if(B(m, n) is not encoded)

ES = AST_Enc(B(m, n));

$if(ES \neq' ZT')$

{

$for\ l = 2\ to\ l\_max$

{

$[K_{void}\ ,\ No\_of\_SC] = scan[P_3]$;

: Function Scan(.) will scan all the coefficients of the spatial tree for detection of zerotree.

$for\ n = 1\ to\ No\_of\_SC$

{

: Encode Significant coefficients

$ES = AST\_Enc[\beta_s(m,n)]$

: Encode position of significant coefficients tree;

$$Z(m,n) = Q_i(m,n)$$

}

}

}

Step4: Bitstream based on coefficients significance:

$$if(|Q[B(m,n)]| > |B(m,n)|)$$
$$Ref\ Bit = 1;$$
$$else$$
$$Ref\ Bit = 0;$$

Step5: Update the Threshold. $T_{adp} = \frac{T_{adp}}{2}$ and repeat step 3.

e. The embedded bit stream is decoded by the Huffman decoder followed by Debouches 4 wavelet reconstruction filters.
f. The optimizer algorithm calculates the finest ranks and threshold using eq. 9 and 10 for both compression sub-blocks.
g. Use inverse SVD for all sub-blocks using Eq. (5) and add the extracted mean value.

4 Quality metrics

There are several metrics available to evaluate the quality of reconstructed image, but in this paper, we use three common error metrics peak signal-to-noise ratio (PSNR), structural similarity index mode (SSIM), and edge-preserving index (EPI) to measure the performance of the proposed algorithm. PSNR is given as,

$$MSE = \frac{1}{MN}\sum_{i,j=1}^{M,N}\left(I_r(m,n) - I_o(m,n)\right)^2 \tag{12}$$

$$PSNR = 10\log_{10}\left(Q^2/MSE\right) \tag{13}$$

Where M, N is the size of the image and I_o is the original image I_r is a reconstructed image, Q is 255 for the grayscale image. Variation of brightness in a reconstructed image amplifies the PSNR values. Measuring only PSNR is not the best choice to evaluate the image quality, therefore we use SSIM as an improved version of PSNR and measures clears the inconsistency in human visual perception. It is defined as [26],

$$SSIM(x,y) = \frac{\left(2\mu_x\mu_y + C_1\right)\left(2\sigma_{xy} + C_2\right)}{\left(\mu_x^2 + \mu_y^2 + C_1\right)\left(\sigma_x^2 + \sigma_y^2 + C_2\right)} \tag{14}$$

x and y correspond to two image blocks that need to be measured,μ_x, $\mu_y$are average and $\sigma_x\sigma_y$are the variance of x, y respectively. σ_{xy} Is the covariance of x and y.$C_1=(K_1L)^2$, *and* $C_2=(K_2L)^2$ Are variables of the stabilization factor. L=dynamic range, $K_1=0.01$, $K_2=0.03$It measures the similarity index of the reconstructed image concerning the original image.

The edge preservation is a quantitative measure, calculated by using the formula for reference grayscale image *I(x,y)*,

$$EPI = \frac{\tau\left(\Delta I - \overline{\Delta I}, \hat{\Delta} I - \overline{\hat{\Delta} I}\right)}{\sqrt{\tau\left(\Delta I - \overline{\Delta I}, \Delta I - \overline{\Delta I}\right)\tau\left(\hat{\Delta} I - \overline{\hat{\Delta} I}, \hat{\Delta} I - \overline{\hat{\Delta} I}\right)}} \tag{15}$$

Where $\hat{I}(m,n)$ is the estimated pixel intensity of the reference image, $\overline{I}(m,n)$ and $\bar{\hat{I}}(m,n)$ are the mean value of the reference image in the region of interest.$\Delta I(m,n)$ is a highpass filtered version of $I(m,n)$, obtain from *the* 3×3 pixel standard estimate of the Laplacian operator [29].

Fig. 4 SVD Compressed block4 Image using different levels of singular values 'S' with Average ranks 'r'

5 Simulation results and discussions

The proposed compression algorithm is evaluated by using standard test images collected from (8-bit grayscale test images) from the SIPI database, which is shown in Fig. 4.

The tabulations in Table 2, 3, 4, 5, 6, 7, 8, 9 and 10 shows a comparative study of the proposed method with EZTW, SPIHT, JPEG, and WDR_SVD in terms of PSNR, SSIM, and EPI at compression ratio 30:1,70:1,90:1 respectively.

Tables 2, 3 and 4 show that the PSNR values of the proposed method are improved from the basic EZTW method and compete with other algorithms. The PSNR value

Table 2 PSNR comparison for fixed CR 30:1

Images	EZTW(DB)	SPIHT(DB)	JPEG(DB)	WDR_SVD(DB)	MEZTW_SVD(DB)
Artificial	27.54	**29.34**	28.43	27.98	28.60
Big_Building	25.95	26.85	27.94	28.67	**28.86**
Boats	28.39	29.27	30.43	31.01	**31.30**
Bridge	27.33	26.35	27.79	28.24	**28.13**
Deer	31.78	38.32	**39.45**	34.78	32.07
Fireworks	34.02	33.29	34.24	**36.09**	**35.09**
Goldhill	28.88	30.20	31.09	30.67	**32.13**
Lena	29.26	33.24	34.77	31.65	32.38
Peppers	30.38	31.28	30.87	30.33	**32.59**

Table 3 PSNR comparison for fixed CR 70:1

Images	EZTW(DB)	SPIHT(DB)	JPEG(DB)	WDR_SVD(DB)	MEZTW_SVD(DB)
Artificial	22.51	25.61	26.42	**27.22**	24.22
Big_Building	21.84	24.02	25.06	**26.41**	24.41
Boats	23.21	26.44	26.59	26.24	**26.70**
Bridge	21.85	23.35	23.54	23.27	**23.45**
Deer	28.48	33.06	**34.73**	34.56	29.20
Fireworks	23.25	25.06	24.69	**27.89**	23.60
Goldhill	24.08	27.42	27.51	26.59	**27.21**
Lena	24.29	29.61	28.32	27.36	**27.45**
Peppers	24.28	**29.66**	28.99	29.21	27.34

of the proposed method for boat image is 0.8 dB, 0.2 dB, and 2 dB higher than the WDR_SVD, JPEG compression technique at compression ratios 30:1, 70:1, and 90:1 respectively.

Tables 5, 6 and 7 shows SSIM values of the proposed method and other algorithms at a compression ratio of 30:1, 70:1, and 90:1. The SSIM value of the proposed method at 30:1 was found satisfactory compared to other algorithm except for deer and Lena images. The deer and fireworks have a rich number of artifacts and compression with high CR value coarsely removes that feature during reconstruction Fig. 5.

However, in Tables 8 and 9, the EPI value of the proposed method is comparatively higher than that of other methods, but images of firework, artificial, etc. have a set of large significant information, and preserving all of them give less EPI. The edge-preserving capacity of the proposed method is retained even at a high compression ratio can be observed in Table 10.

Figure 6 shows a graphical comparison of the proposed method with the art of work for Boat images in terms of PSNR, SSIM, and CR. This graphical comparison shows that the PSNR and SSIM of the proposed method compete with other algorithms in achieving high reconstruction quality.

Table 4 PSNR comparison for fixed CR 90:1

Images	EZTW(DB)	SPIHT(DB)	JPEG(DB)	WDR_SVD(DB)	MEZTW_SVD(DB)
Artificial	20.34	21.94	**23.78**	23.54	22.03
Big_Building	18.34	20.96	20.75	20.03	**21.23**
Boats	21.16	23.07	22.12	23.65	**24.69**
Bridge	19.14	20.45	20.34	20.09	**21.23**
Deer	24.18	27.46	25.09	24.98	**25.13**
Fireworks	19.44	**24.39**	22.14	19.67	19.61
Goldhill	21.85	24.24	24.32	24.63	**24.99**
Lena	21.24	24.94	24.98	24.73	**24.75**
Peppers	20.87	24.74	24.66	23.99	**24.08**

Table 5 SSIM values for fixed CR 30:1

Images	EZTW	SPIHT	JPEG	WDR_SVD	MEZTW_SVD
Artificial	0.845	0.818	0.819	0.839	**0.846**
Big_Building	0.768	0.712	0.733	0.746	**0.767**
Boats	0.802	0.789	0.763	0.799	**0.806**
Bridge	0.862	0.828	0.852	**0.865**	0.841
Deer	0.907	0.957	0.942	**0.965**	0.908
Fireworks	0.924	0.892	0.904	0.901	**0.932**
Goldhill	0.820	0.776	0.791	0.818	**0.821**
Lena	0.867	**0.881**	0.868	0.832	0.858
Peppers	0.893	0.785	0.799	0.789	**0.880**

5.1 Computational complexity

The extraction of the mean from the image increases inter-pixel relation and partition of the image into subblocks for SVD to enhance coding efficiency and time reductional process. The steps in level two compression using adaptive specific ranks in SVD and encoding of blocks in MEZTW with significance mapping for adaptive thresholds are an addon for this algorithm. There is an uncertainty between reconstruction quality PSNR and bit per pixel (BPP) since high PSNR favor a larger number of encoding bit stream. Hence, the computational cost is associated with the range of significant mapping in MEZTW and the optimization process. This algorithm attempts to reduce the range of embedded bit stream with the optimal threshold at a high compression rate of 90 but, a smaller bitstream affected the quality of the decoded image and SSIM.

It is shown in Fig. 7. The firework image is compressed by the proposed method at compression ratios 30:1, 70:1, and 90:1 respectively. In Fig. 8 the boat image is compressed by using EZTW, SPIHT, JPEG, and the proposed method at a fixed compression ratio of 50:1. From Fig. 8 we can observe the perceptual quality of the reconstructed image by the proposed compression algorithm is efficient and improved from basic EZTW algorithm.

Table 6 SSIM values for fixed CR 70:1

Images	EZTW	SPIHT	JPEG	WDR_SVD	MEZTW_SVD
Artificial	0.519	**0.690**	0.664	0.658	0.621
Big_Building	0.522	0.577	**0.594**	0.556	0.525
Boats	0.573	**0.676**	0.655	0.635	0.576
Bridge	0.616	**0.711**	0.705	0.709	0.619
Deer	0.786	0.920	0.912	0.774	0.787
Fireworks	0.620	0.772	0.694	0.723	0.778
Goldhill	0.537	**0.668**	0.523	0.511	0.537
Lena	0.656	**0.804**	0.798	0.605	0.646
Peppers	0.695	0.753	0.656	0.666	**0.695**

Table 7 SSIM values for fixed CR 90:1

Images	EZTW	SPIHT	JPEG	WDR_SVD	MEZTW_SVD
Artificial	0.371	0.512	0.440	0.475	**0.542**
Big_Building	0.372	0.421	0.463	0.475	0.380
Boats	0.478	0.540	0.490	0.489	**0.568**
Bridge	0.491	0.548	0.498	0.499	**0.569**
Deer	0.734	**0.842**	0.759	0.766	0.745
Fireworks	0.545	0.671	0.643	0.654	**0.742**
Goldhill	0.447	0.544	**0.581**	0.533	0.450
Lena	0.565	**0.682**	0.564	0.587	0.568
Peppers	0.580	**0.638**	0.632	**0.646**	0.590

Table 8 EPI values for fixed CR 30:1

Images	EZTW	SPIHT	JPEG	WDR_SVD	MEZTW_SVD
Artificial	32.6	34.8	**39.7**	36.4	37.0
Big_Building	33.4	36.9	**44.2**	40.0	39.3
Boats	30.3	29.2	34.6	34.7	**35.3**
Bridge	41.5	40.9	41.8	**40.7**	**42.1**
Deer	44.5	43.8	47.8	**45.6**	**48.0**
Fireworks	26.7	28.6	**32.2**	**31.7**	30.4
Goldhill	30.6	33.2	33.4	32.9	**33.6**
Lena	41.5	42.1	**45.7**	**44.7**	44.9
Peppers	48.8	49.2	50.3	52.3	**53.7**

Table 9 EPI values for fixed CR 70:1

Images	EZTW	SPIHT	JPEG	WDR_SVD	MEZTW_SVD
Artificial	20.2	23.4	24.6	23.9	**24.7**
Big_Building	26.2	26.7	29.0	28.8	**30.4**
Boats	28.4	28.5	28.8	29.7	**30.2**
Bridge	30.5	30.9	32.3	31.8	**33.1**
Deer	33.6	32.6	33.9	34.3	**34.7**
Fireworks	20.6	21.4	**24.1**	23.6	22.8
Goldhill	20.6	19.4	20.4	20.8	**21.4**
Lena	31.1	32.2	**35.6**	33.6	34.9
Peppers	35.9	32.4	36.6	37.1	**38.3**

Table 10 EPI values for fixed CR 90:1

Images	EZTW	SPIHT	JPEG	WDR_SVD	MEZTW_SVD
Artificial	10.3	9.9	11.4	12.2	**15.4**
Big_Building	12.2	15.4	19.7	18.9	**20.5**
Boats	13.6	17.1	20.4	24.6	**26.8**
Bridge	20.5	23	25.1	24.5	**25.6**
Deer	18.4	20.1	22.5	22.3	**22.8**
Fireworks	7.4	6.5	14.3	16.2	**16.7**
Goldhill	16.6	19.4	20.4	19.8	**20.6**
Lena	19.7	20.3	21.6	20.4	**22.8**
Peppers	13.6	15.5	18.7	19.3	**21.4**

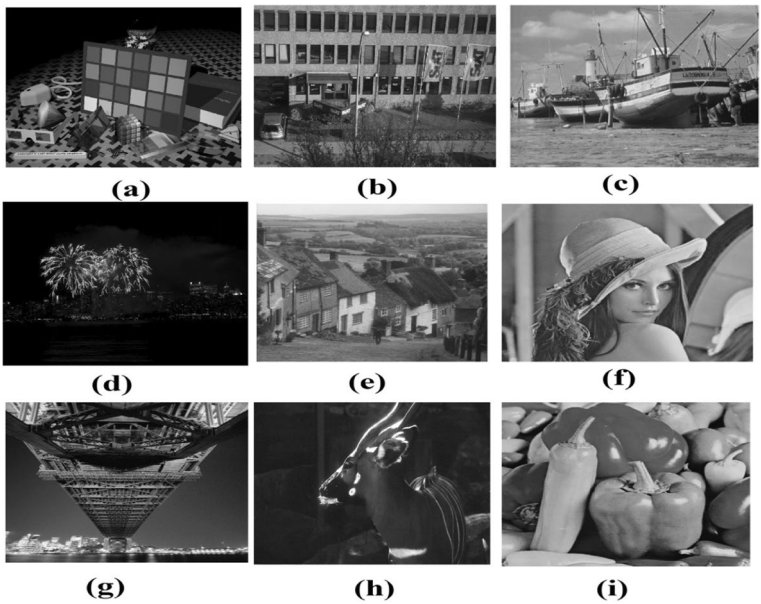

Fig. 5 Test images (**a**)Artificial; (**b**)Big_building; (**c**)Boat; (**d**)Fireworks; (**e**)Goldhills; (**f**)Lena; (**g**) Bridge; (**h**)Deer; (**i**)Pepper

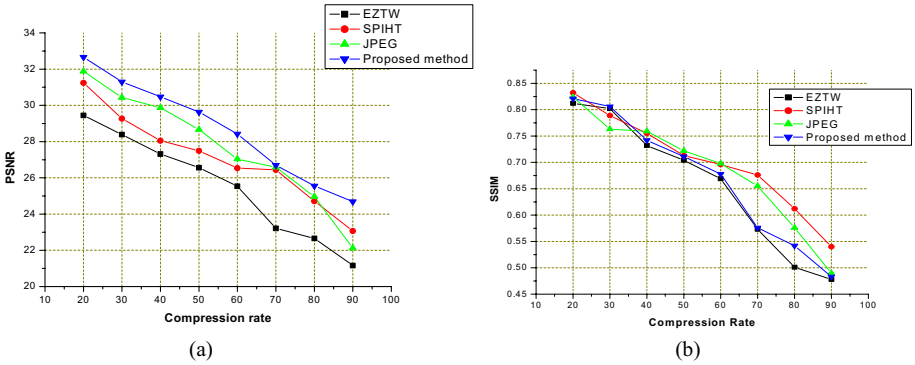

Fig. 6 Graphical comparison of the proposed method with the art of work in terms of PSNR, SSIM v/s Compression ratio, (**a**) PSNR v/s Compression ratio, (**b**) SSIM V/s Compression ratio

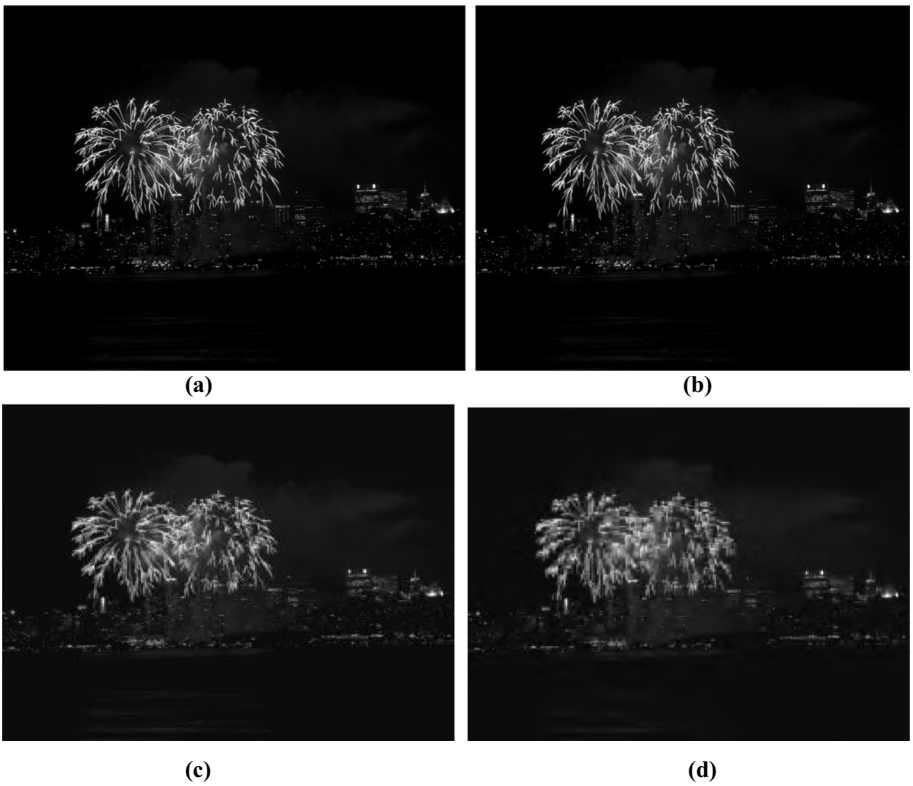

Fig. 7 **a** Uncompressed fireworks image is compressed by compression ratios of (**b**) 30:1; (**c**) 70:1; (**d**) 90:1 using segmentation-based rank one updated SVD_EZTW method

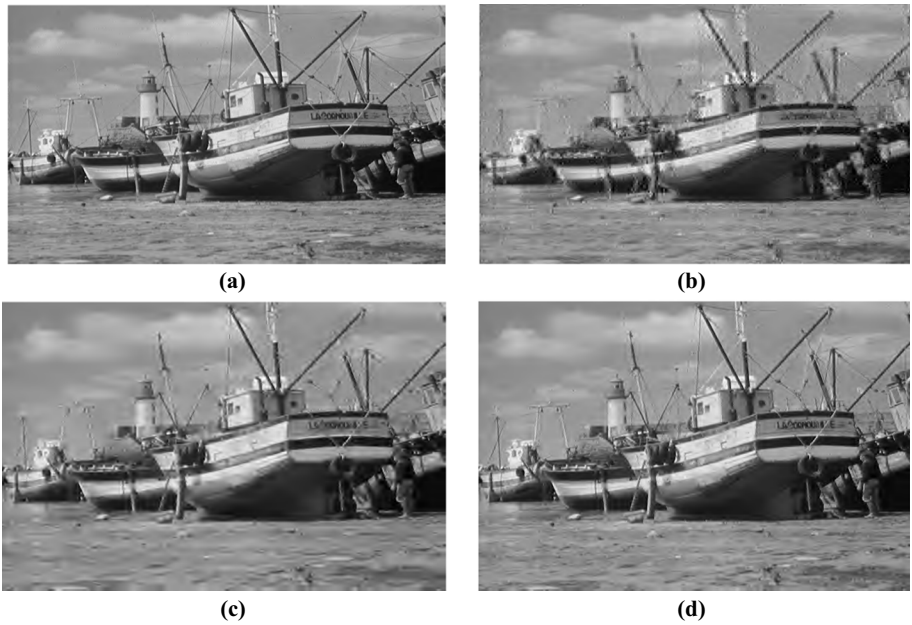

Fig. 8 Original Boat image compressed by (**a**) EZTW; (**b**) Basic SPIHT; (**c**) JPEG; (**d**) proposed method at compression rate 50:1

6 Conclusion

The scaled SVD and EZTW are progressive image compressions that found significant improvement from current compression algorithms. The above result and discussion show this algorithm is an efficient image compression method for multimedia image compression applications. The determination of the advanced level of spots in SVD and low bit rate coding in MEZTW improves the PSNR estimation at a fixed compression rate. The one significant improvement we observed in this algorithm is at a high compression rate the image quality preservation was not worse than other algorithms. Even though the SSIM performance of the proposed technique is less contrasted with SPIHT and JPEG at a high compression ratio. Since in MEZTW compression at a high compression ratio, the unwanted image information is eliminated, even a few significant sub-bands were also neglected for low bit rate transmission. This algorithm efficiency can be enhanced by reducing time complexity at the point of segmentation and optimizer by using a neural network to compute the average ranks and thresholds. This technique effectively preserves edge information even at a high compression rate. In general, the proposed technique fundamentally improves the traditional way of the EZTW algorithm and is also relatively higher than SPIHT and JPEG aside from some points.

Funding The author did not receive financial support from any organization for the submitted work.

Data availability The datasets generated during and/or analyzed during the current study are available in the **SIPI Image Database** repository, [SIPI Image Database - Misc (usc.edu)].

Declarations

Conflict of Interest The authors declare that he has no conflict of interest.

References

1. Internet usage statistics - The Internet Big Picture2023 Updated June 30, 2022; Accessed June 30, 2022, Bogota, Colombia Enrique de Argaez Available at: http://www.internetworldstats.com/stats.htm.
2. Gupta P, Shah D, Bedi N, Galagali P, Dalwai S, Agrawal S, John JJ, Mahajan V, Meena P, Mittal HG (2022) Indian Academy of Pediatrics Guidelines on Screen Time and Digital Wellness in Infants, Children and Adolescents. Indian Pediatr 59:235–244
3. Dua Y, Kumar V, Singh RS (2021) Parallel lossless HSI compression based on RLS filter. J Parallel Distribut Comput 150:60–68
4. Sengupta A, Roy D (2018) Intellectual Property-Based Lossless Image Compression for Camera Systems [Hardware Matters]. IEEE Cons Electron Mag 7(1):119–124
5. Shapiro JM (1993) Embedded Image Coding Using Zerotrees of Wavelet Coefficients. IEEE Trans Signal Proc 41(I2)
6. Liu X, An P, Chen Y (2022) An improved lossless image compression algorithm based on Huffman coding. Multimed Tools Appl 81:4781–4795
7. Mishra D, Singh SK, Singh RK (2022) Deep Architectures for Image Compression: A Critical Review. Signal Process 191:1–27
8. Li D, Wu S, Jiao J, Zhang Q (2019) Compressed Image Sensing by Jointly Leveraging Multi-Scale Heterogeneous Priors for the Internet of Multimedia Things, in IEEE. Access 7:18915–18925
9. Wu S, Zhang T, Jiao J, Yang J, Zhang Q (2017) Statistical prior aided separate compressed image sensing for the green Internet of multimedia things, Mobile. Inf Syst 9. https://doi.org/10.1155/2017/2314062
10. Bhardwaj D, Pankajakshan V (2018) A JPEG blocking artifact detector for image forensics. Signal Process Image Commun 68:155–161
11. Said A, Pearlman WA (1996) A new, fast and efficient image codec based on set partitioning in hierarchical trees. IEEE Trans Circuits Syst Vid technology,6(3):243–250
12. Taubman D (2000) High-performance scalable image compression with EBCOT. IEEE Trans Image Process 9(7):1158–1170
13. Kumar M, Vaish A (2016) An efficient compression of encrypted images using WDR coding,(436), pp. 729–741.
14. J.S. Walker, T.O. Nguyen, (2001) Adaptive scanning methods for Wavelet difference reduction in lossy image compression, International conference on image processing IEEE process;(3); pp. 22-35.
15. Hou ZJ (2003) Adaptive singular value decomposition in wavelet domain for image denoising. Pattern Recogn 36(8):1747–1763
16. Tian GJ (2015) Combination of SVD and Wavelet Transform for Oil Discrimination on 3-D Fluorescence Spectra. Appl Mech Mater 740:639–643
17. Zear A, Singh AK, Kumar P (2018) A proposed secure multiple watermarking technique based on DWT, DCT, and SVD for application in medicine. Multimed Tools Appl 77(4):4863–4882
18. Ranjeeth Kumar A, Kumar GK, Singh. (2016) A hybrid method based on singular value decomposition and embedded zero tree wavelet technique for ECG signal compression. J Comput Methods, Prog Biomed 129:135–148
19. Wang Y, Yang Y (2022) Hot-SVD: higher-order t-singular value decomposition for tensors based on tensor–tensor product. Comput Appl Math 41(394)
20. Andrews HC, Patterson CL Singular value decompositions, and digital image processing. IEEE Trans Acous, Speech Sig Proc 1(24):26–53
21. Rufai AM, Anbarjafari G, Demirel H (2014) Lossy image compression using singular value decomposition and wavelet difference reduction. Dig Sig Proc 24:117–123
22. Rasti P, Daneshmand M (2015) Resolution Enhancement Based Image Compression Technique using Singular Value Decomposition and Wavelet Transforms. Intech publication, Wavelet Transform and Some of Its Real-World Applications, pp 36–51
23. Bekar CG, Gallivan KA, P.Van Dooren, (2012) Low-Rank incremental methods for computing dominant singular subspaces, Linear Algebra and its Application, Elsevier pub (432); pp.2866–2888
24. Chen J, (2000) Image compression with SVD, ECS 29K, Scientific computation, Available: http://fourier.eng.hmc.edu/e161/lectures/svdcompression.html#Aase99
25. Kiwon Y, Han C, Kang U, Sohan K (2011) Embedded compression algorithm using error aware quantization and hybrid DPCM/BTC coding. IEEE Int Conf Multimed Expo (ICME):1–6

26. Boujelbene R, Boubchir L, Jemaa YB (2019) Enhanced embedded zero tree wavelet algorithm for lossy image coding. IET Image Process 13(8):1364–1374
27. Ahmadi K, Javaid AY, Salari E (2015) An efficient compression scheme based on adaptive thresholding in wavelet domain using particle swarm optimization. J Signal Proc: Imag Commun 32:33–39
28. Wen J, Wang J, Zhang Q (2017) Nearly optimal bounds for orthogonal least squares. IEEE Trans Signal Process 65(20):5347–5356
29. Burt PJ, Adalson EH, (1983) The Laplacian pyramid as a compact image code, IEEE Trans Commun :(31), pp.532-540